THE JOURNAL OF BIOLOGICAL CHEMISTRY VOL. 284, NO. 12, pp. 7756–7765, March 20, 2009

Novel Determinants of Epithelial Sodium Channel Gating within Extracellular Thumb Domains*

Received for publication, September 11, 2008, and in revised form, January 15, 2009 Published, JBC Papers in Press, January 21, 2009, DOI 10.1074/jbc.M807060200

Ahmad B. Maarouf[‡1], Nan Sheng[‡], Jingxin Chen[‡], Katie L. Winarski[‡], Sora Okumura[‡], Marcelo D. Carattino[‡], Cary R. Boyd[‡], Thomas R. Kleyman[‡§2], and Shaohu Sheng[‡3]

From the [‡]Renal-Electrolyte Division, Department of Medicine, and the [§]Department of Cell Biology and Physiology, School of Medicine, University of Pittsburgh, Pittsburgh, Pennsylvania 15261

Activity of the epithelial Na^+ channel (ENaC) is modulated by Na^+ self-inhibition, an allosteric down-regulation of channel open probability by extracellular Na^+. We searched for determinants of Na^+ self-inhibition by analyzing changes in this inhibitory response resulting from specific mutations within the extracellular domains of mouse ENaC subunits. Mutations at γMet^{438} altered the Na^+ self-inhibition response in a substitution-specific manner. Fourteen substitutions (Ala, Arg, Asp, Cys, Gln, Glu, His, Ile, Phe, Pro, Ser, Thr, Tyr, and Val) significantly suppressed Na^+ self-inhibition, whereas three mutations (Asn, Gly, and Leu) moderately enhanced the inhibition. Met to Lys mutation did not alter Na^+ self-inhibition. Mutations at the homologous site in the α subunit (G481A, G481C, and G481M) dramatically increased the magnitude and speed of Na^+ self-inhibition. Mutations at the homologous βAla^{422} resulted in minimal or no change in Na^+ self-inhibition. Low, high, and intermediate open probabilities were observed in oocytes expressing αG481M$\beta\gamma$, $\alpha\beta\gamma$M438V, and αG481M/$\beta\gamma$M438V, respectively. This pair of residues map to the α5 helix in the extracellular thumb domain in the chicken acid sensing ion channel 1 structure. Both residues likely reside near the channel surface because both αG481C$\beta\gamma$ and $\alpha\beta\gamma$M438C channels were inhibited by an externally applied and membrane-impermeant sulfhydryl reagent. Our results demonstrate that αGly^{481} and γMet^{438} are functional determinants of Na^+ self-inhibition and of ENaC gating and suggest that the thumb domain contributes to the channel gating machinery.

Maintenance of body fluid volume homeostasis requires a collaborative interaction of many Na^+ transport mechanisms. Na^+ transport in epithelia that line the late distal convoluted tubule, connecting tubule, and collecting tubule relies on apical Na^+ entry through epithelial Na^+ channels (ENaC).[4] Gain-of-function and loss-of-function ENaC mutations in humans result in Liddle syndrome and pseudohypoaldosteronism type I, respectively (1). ENaC activity is regulated by a variety of factors that primarily alter channel density at plasma membrane, open probability (P_o), or both. ENaC gating is characterized by long open and close time in the range of up to minutes and a highly variable P_o, although channels with brief open (on the order of tens of ms) and long close times have also been observed (2, 3). Although previous studies have identified several regions that appear to have a role in ENaC gating, the mechanism of ENaC gating is not well understood. It is now well established that ENaC undergoes a reduction in P_o as a result of Na^+ binding to extracellular component(s) within the channel complex, a process referred to as Na^+ self-inhibition (4–6). Recent studies have revealed specific characteristics and have identified several sites that have a functional role in Na^+ self-inhibition (4, 6–8). However, detailed elements regarding its mechanism have not been revealed.

A logical place to search for structural elements associated with Na^+ self-inhibition is the large extracellular domain (ECD) that connects the two transmembrane domains (M1 and M2) within each ENaC subunit. The ECD likely exists as well structured subdomains with 16 conserved Cys residues. We recently reported that point mutations at multiple α and γ ECD Cys residues blunted Na^+ self-inhibition, and certain double or triple mutations rendered ENaC insensitive to high concentration of extracellular Na^+. These results suggest that multiple Cys residues are required to establish the proper tertiary structure permitting this allosteric regulation (9). In addition, the N-terminal portion of ECD contains γHis^{239}, a previously identified residue critical for Na^+ self-inhibition, as well as defined protease cleavage sites (4, 10–12). Various proteases have been shown to regulate ENaC activity, in part, by interfering with Na^+ self-inhibition (6, 7, 13).

The resolved high resolution structure of the chicken acid-sensing ion channel 1 (cASIC1) revealed an extracellular domain with a highly organized structure characterized by β sheets within a core embedded within peripheral α helices (14). These helices form the finger, thumb, and knuckle domains, whereas two bundles of long and short β-sheets occupy the palm and β-ball domains. Given the similarities in amino acid sequences and biophysical properties among ASIC and other members of ENaC/degenerin family, it is very likely that ENaC

* This work was supported, in whole or in part, by National Institutes of Health Grant R01 DK054354, R01 ES014701, and P30 DK079307. The costs of publication of this article were defrayed in part by the payment of page charges. This article must therefore be hereby marked "*advertisement*" in accordance with 18 U.S.C. Section 1734 solely to indicate this fact.

[1] Supported by a postdoctoral fellowship award from the American Heart Association.

[2] To whom correspondence may be addressed: Renal-Electrolyte Division, University of Pittsburgh, 3550 Terrace St., Pittsburgh, PA 15261. Tel.: 412-647-3121; Fax: 412-383-8956; E-mail: kleyman@pitt.edu.

[3] To whom correspondence may be addressed: Renal-Electrolyte Division, University of Pittsburgh, 3550 Terrace St., Pittsburgh, PA 15261. Tel.: 412-647-3121; Fax: 412-383-8956; E-mail: shaohu@pitt.edu.

[4] The abbreviations used are: ENaC, epithelial Na^+ channel; ECD, extracellular domain; WT, wild type; MTSET, 2-(Trimethylammonium) ethyl methanethiosulfonate bromide; cASIC, chicken acid-sensing ion channel; cRNA, complementary RNA.

subunits adopt a similar overall tertiary structure, although considerable differences likely exist within local structures, particularly for poorly conserved regions that likely contribute to differences in the biophysical properties of ASIC and ENaC. Additional evidence supporting the notion that ECDs of ASIC and ENaC share a similar overall structure is that the disulfide bridges proposed for the ECD of α ENaC, based on mutational analyses and chemical modifications, match the disulfide bonds within the cASIC1 structure (9, 14).

In searching for additional determinants for Na^+ self-inhibition and ENaC gating, we observed a significant suppression of this inhibitory response by a mutation of a Met residue (M438A) within the second cysteine-rich domain in ECD of γENaC. The γMet^{438} is near the 13th conserved Cys (γCys^{440}) whose mutation leads to significant suppression of Na^+ self-inhibition (9). Sequence alignments placed this residue at a site corresponding to Lys^{342} within cASIC1, which is located at the N-terminal part of helix α5, one of the two helices that comprise the thumb domain (Fig. 1). The thumb domain within cASIC1 was proposed to interact with other parts of the extracellular domains during proton gating of the channel (14). In this study we performed mutagenesis analyses to assess the functional role of γMet^{438} and its homologous residues in α and β ENaC in Na^+ self-inhibition.

EXPERIMENTAL PROCEDURES

Site-directed Mutagenesis and in Vitro Transcription—Mouse α, β, and γ ENaC cDNAs in pBluescript SK- vector (Stratagene, La Jolla, CA) were used as templates to generate point mutations using a PCR-based method as previously described (15). Target mutations were confirmed by direct sequencing. The complementary RNAs (cRNAs) for wild type (WT) and mutant ENaC subunits were synthesized with T3 RNA polymerase (Ambion, Inc.), purified with an RNA purification kit (Qiagen Inc., Valencia, CA), and quantitated by spectrophotometry and density analyses of the RNA band in a denaturing agarose gel.

ENaC Expression and Two-electrode Voltage Clamp—ENaC expression in *Xenopus* oocytes and current measurements by two-electrode voltage clamp were performed as previously reported (15). Defolliculated oocytes were injected with 50 nl/cell of mixed cRNAs containing 1 ng of cRNA for each mENaC subunit (α, β, and γ) and incubated at 18 °C in modified Barth's saline (88 mM NaCl, 1 mM KCl, 2.4 mM $NaHCO_3$, 15 mM HEPES, 0.3 mM Ca $(NO_3)_2$, 0.41 mM $CaCl_2$, 0.82 mM $MgSO_4$, 10 μg/ml sodium penicillin, 10 μg/ml streptomycin sulfate, 100 μg/ml gentamycin sulfate, pH 7.4). All of the experiments were performed 20–50 h following cRNA injections at room temperature (20–24 °C). The oocytes were placed in an oocyte recording chamber from Warner Instruments (Hamden, CT) and perfused with constant flow rate of 12–15 ml/min. Voltage clamp was performed using TEV-200 Voltage Clamp amplifier (Dagan Corp.) and DigiData 1322A interface controlled by pClamp 9 (Molecular Devices Corporation, Sunnyvale, CA).

Procedures for Observing Na^+ Self-inhibition—To examine Na^+ self-inhibition, a low Na^+ bath solution (NaCl-1; containing 1 mM NaCl, 109 mM *N*-methyl-D-glucamine, 2 mM KCl, 2 mM $CaCl_2$, 10 mM HEPES, pH 7.4) was replaced rapidly by a high Na^+ bath solution (NaCl-110; containing 110 mM NaCl, 2 mM KCl, 2 mM $CaCl_2$, 10 mM HEPES, pH 7.4), whereas the oocytes were continuously clamped to −60 or −100 mV as indicated. Bath solution exchange was performed with a 6-channel Teflon valve perfusion system from Warner Instruments. At the end of the experiment, 10 μM amiloride was added to the bath to determine the amiloride-insensitive component of the whole cell current. Currents remaining in the presence of 10 μM amiloride were generally less than 200 nA. The results from oocytes that showed unusually large amiloride-insensitive currents (>5% of total currents) were discarded to minimize current contamination from endogenous channels and membrane leak. Given the well known variability of *Xenopus* oocyte expression system and our initial observation that the Na^+ self-inhibition responses of WT αβγ mENaCs varied moderately among different batches of oocytes, despite a very small variation in the response within the same batch of oocytes, the responses of WT channels were always examined with mutants in the same batch of oocytes in an alternating manner.

The first 40 s of current decay was fit with an exponential equation by Clampfit 9.0 (Axon Instruments Inc.). The peak current (I_{peak}) was the measured maximal inward current immediately after bath solution exchange from low Na^+ to high Na^+ concentration. The steady state current (I_{ss}) represented the measured current at 40 s post I_{peak}. The current ratio of I_{ss}/I_{peak} was calculated from amiloride-sensitive I_{ss} and I_{peak} obtained by subtracting amiloride-insensitive currents from I_{ss} and I_{peak}.

Analysis of Na^+ Binding Affinity—To estimate the Michaelis constant (K_m) for the Na^+ concentration-current relationship, both I_{peak} and I_{ss} were measured in the same cell after the bath Na^+ concentration was raised from 1 to 3, 10, 30, 60, 90, or 110 mM. I_{peak} and I_{ss} were plotted against $[Na^+]$. K_m and V_{max} (maximal current) were obtained by best fit of the current-concentration data according to the following equation, with least squares nonlinear curve fitting using Origin Pro 7.5 (OriginLab Corporation, Northampton, MA): $I = V_{max} \cdot C/(C + K_m)$. In the equation, I is the relative I_{peak} or I_{ss}, and C refers to the $[Na^+]$ used to initiate self-inhibition. The apparent inhibitory constant (K_i) of Na^+ self-inhibition was estimated by fitting I_{ss} and $[Na^+]$ data with an equation for substrate inhibition of enzymes (16): $I_{ss} = V_{max} \cdot C/(K_m + C + C^2/K_i)$.

Single Channel Recordings—The oocytes were placed in a hypertonic solution (NaCl-110 supplemented with 200 mM sucrose) for 5 min, and the vitelline membranes were removed manually. The oocytes were then transferred to a recording chamber with NaCl-110 and maintained for at least 20 min at room temperature (22–25 °C) before recordings. Pipette solution was the same as bath solution (NaCl-110). Patch pipettes with a tip resistance of 5–10 MΩ were used. Patch clamp in the cell-attached configuration was performed using PC-One Patch Clamp amplifier (Dagan Corp.) and a DigiData 1322A interface connected to a PC. The patches were clamped at membrane potentials (negative value of pipette potentials) of −40 to −100 mV. Software pClamp 8 or 10 (Molecular Devices Corporation) was used for data acquisition and analyses. Single channel recordings were acquired at 5 kHz, filtered at 300 Hz by

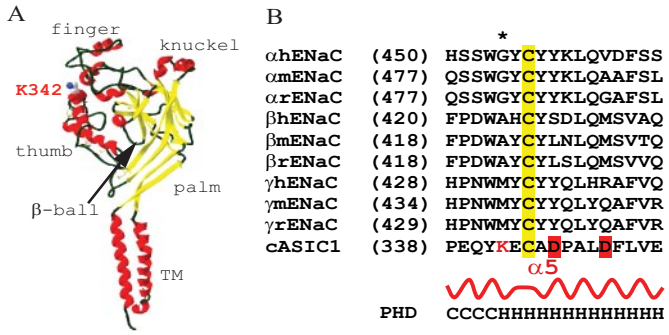

FIGURE 1. **Location of αGly^{481}/γMet^{438}.** *A*, structure of chain A of cASIC1 is drawn from Protein Data Bank coordinates (2QTS) with a DeepView/Swiss-PDB-Viewer v3.7. Solvent molecules and the bound chloride ion are not shown. Backbone is shown in ribbons with coloring according to secondary structures: helix in *red*, β-sheet in *yellow*, and coiled in *dark green*. Residue Lys^{342} is displayed in the CPK color scheme and labeled. *B*, sequence alignments of human (*h*), mouse (*m*), and rat (*r*) ENaC subunits and cASIC1 were performed with Vector NTI v10 (Invitrogen), and only the α5 regions are shown. The sequence numbers of the first residues in the alignments are shown in *parentheses*. Lys^{342} is shown a *red letter K*, and the potential proton binding sites are *highlighted* in *red*. The *asterisk* identifies αGly^{481}, βAla^{422}, and γMet^{438} in mENaC studied in this report. Secondary structures from cASIC1 (Protein Data Bank code 2QTS) and predicted for ENaCs by PHD (profile network from Heidelberg) algorithm are shown in curve and letters (*C* for coiled and *H* for helical), respectively.

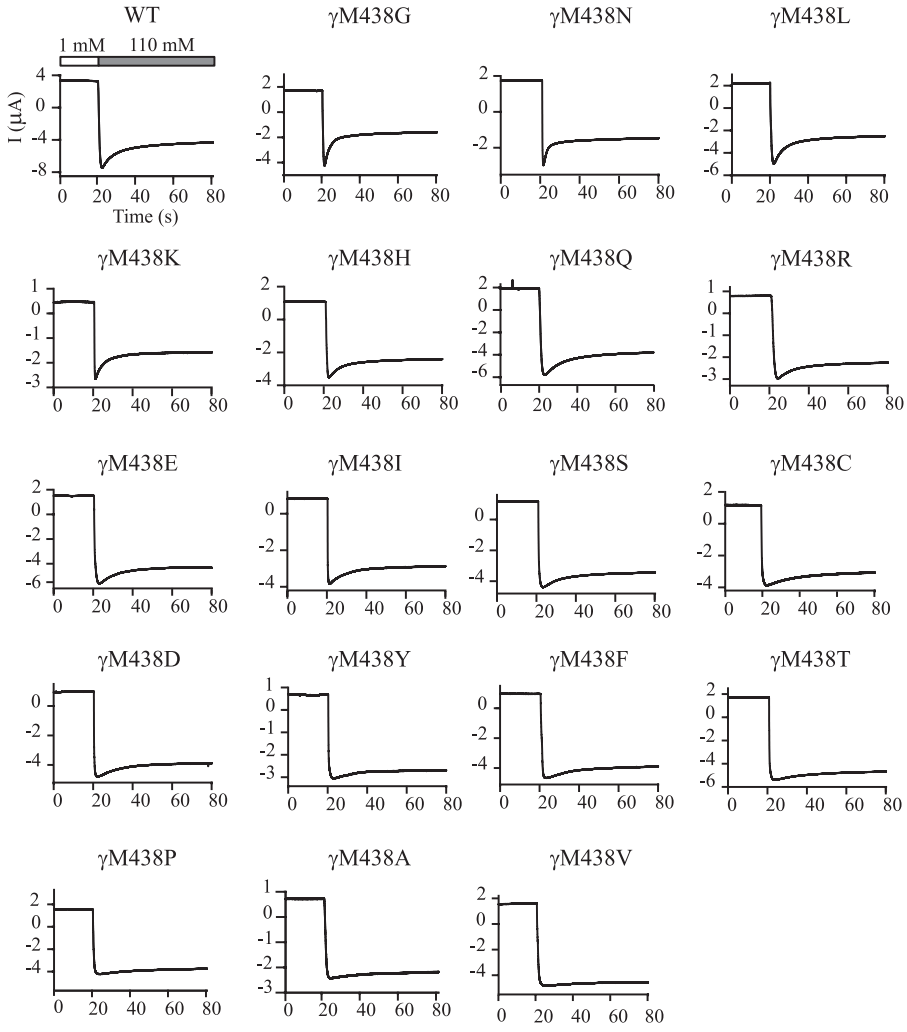

FIGURE 2. **Mutations of γMet^{438} alter the Na$^+$ self-inhibition response.** The oocytes were clamped at −60 mV and whole cell currents were continuously recorded whereas bath [Na$^+$] was rapidly increased from 1 mM (*open bar*) to 110 mM (*gray bar*). The units of current and time for the mutants are the same as for WT αβγ and are omitted for clarity. The *traces* are representative of at least six independent observations.

a 4-pole low pass Bessel Filter built in the amplifier, and stored on the hard disk. Open probability was estimated by single channel search function of pClamp 10 from recordings that contained no more than three current levels at a clamping membrane potential of −100 mV and lasted for at least 2 min. The voltages were not corrected by the junction potential.

Chemicals—2-(Trimethylammonium) ethyl methanethiosulfonate bromide (MTSET) was from Toronto Research Chemicals Inc. All of the other reagents were from Sigma. MTSET was aliquoted in powder and dissolved in bath solution immediately prior to application to avoid hydrolysis.

Statistical Analysis—The data are presented as the means ± S.E. Significance comparisons between groups were performed with *Student's t* tests. A *p* value of less than 0.05 was considered statistically different.

RESULTS

Residue γMet^{438} is not well conserved in ENaC subunits or other ENaC/degenerin members, although its neighboring residues are conserved at a similar degree to the overall homology among ENaC subunits (~35%; Fig. 1*B*). Its corresponding residues are Gly in α, Ala in β, and Lys in most ASIC isoforms. The region harboring γMet^{438} aligns to a helix (α5) within the thumb domain of cASIC1 (Fig. 1*A*), where its homologous residue is Lys^{342} (Fig. 1*A*). We examined the potential role of γMet^{438} and its counterparts in the α and β subunits in Na$^+$ self-inhibition and ENaC gating by analyzing αβγ mouse ENaCs with introduced point mutations.

Mutations at γMet^{438} Alter the Na$^+$ Self-inhibition Response in a Residue-dependent Manner—γMet^{438} was mutated to 18 different amino acids. Co-expression of all mutant mouse γENaC subunits with WT mouse α and β subunits in oocytes resulted in measurable amiloride-sensitive currents permitting examination of Na$^+$ self-inhibition. As shown in Figs. 2 and 3, most substitutions of γMet^{438} (Gln, Arg, Glu, Ile, Ser, Cys, Asp, Tyr, Phe, Thr, Pro, Ala, and Val) greatly suppressed Na$^+$ self-inhibition as determined by the magnitude (I_{ss}/I_{peak}) and rate (tau) of this process ($p < 0.01$). A His residue at this site slightly reduced the magnitude of Na$^+$ self-inhibition ($p < 0.05$), whereas a Leu slightly enhanced the inhibition ($p < 0.05$). Two mutations (γM438G and γM438N) significantly enhanced Na$^+$ self-inhibition ($p < 0.01$). The only mutation

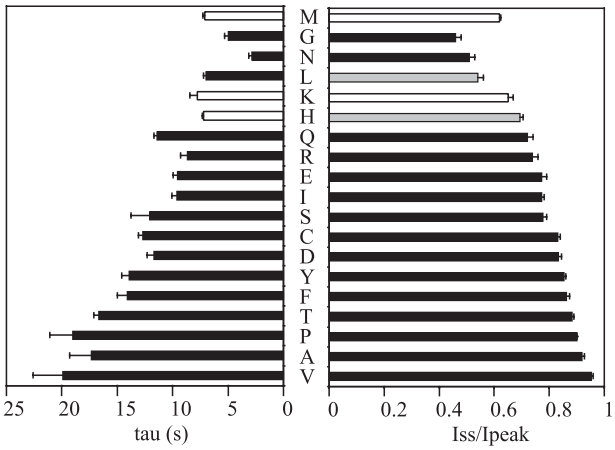

FIGURE 3. **Time constants and magnitude of Na^+ self-inhibition for the γMet^{438} mutants.** The time constants (*left panel*) and I_{ss}/I_{peak} (*right panel*) values were obtained as described under "Experimental Procedures." The data were collected in different batches of oocytes. The WT ($\alpha\beta\gamma$) values represent 111 observations from 16 batches of oocytes, whereas mutant data are from 6–12 oocytes. Student's *t* tests were performed in the same batch of oocytes to compare the Na^+ self-inhibition responses of WT and an individual mutant. Values that are significantly different from that of WT are shown as *black bars* ($p < 0.01$) or *gray bars* ($p < 0.05$).

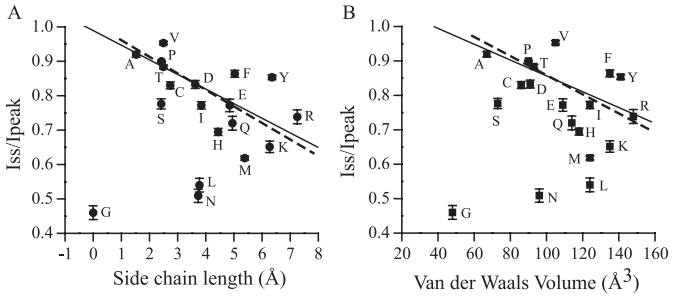

FIGURE 4. **Relationships between side chain length or residual volume and the magnitude of Na^+ self-inhibition.** The I_{ss}/I_{peak} values from Fig. 3 were plotted against either side chain lengths (*A*) or Van der Waals' volumes (*B*) of residues at γ438. Side chain lengths used in the plot were as follows (Å): Gly (0), Ala (1.53), Ser (2.42), Cys (2.74), Pro (2.43), Asp (3.63), Thr (2.49), Asn (3.73), Val (2.49), Gl (4.85), Gln (4.95), His (4.44), Met (5.38), Leu (3.78), Ile (3.84), Lys (6.27), Phe (5.03), Tyr (6.36), and Arg (7.25). The mutants are denoted by single-letter code in the figure. The *solid lines* were from linear fitting of all data points ($n = 19$), and the *dashed lines* were from fitting all data points except Gly ($n = 18$). The weighted linear regression was obtained with Origin Pro 7.5 using weighting factor of 1/S.E. Correlation coefficients were all statistically significant at level of 0.05 except the *solid line* in (*B*, $p = 0.06$).

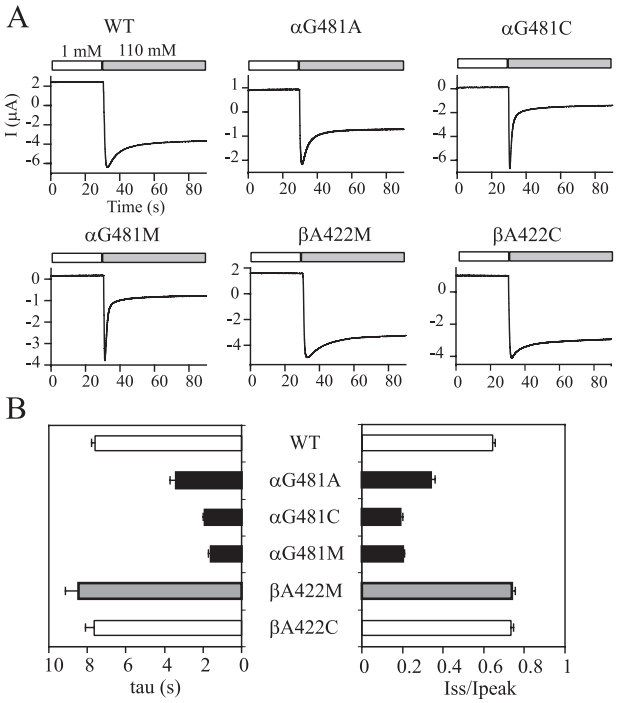

FIGURE 5. **Mutations at αGly^{481} enhance Na^+ self-inhibition.** *A*, representative recordings. The oocytes were clamped at −60 mV, and whole cell currents were continuously recorded, whereas bath [Na^+] was rapidly increased from 1 mM (*open bar*) to 110 mM (*gray bar*). The units of current and time for the mutants are the same as for WT $\alpha\beta\gamma$ and are omitted for clarity. The traces are representative of at least six independent observations. In (*B*), WT data were collected from 44 oocytes derived from eight batches and the mutants from 6–20 oocytes. Student's *t* tests were performed using data obtained with the same batch of oocytes to compare the Na^+ self-inhibition responses of WT and individual mutants. Values that are significantly different from that of WT are shown as *solid bars* ($p < 0.01$) or *gray bars* ($p < 0.05$).

that did not significantly alter the speed and magnitude of Na^+ self-inhibition was γM438K. The data from 19 different channels offered an opportunity to identify residue factors dictating the degree of Na^+ self-inhibition using correlation analysis. A plot of I_{ss}/I_{peak} against side chain lengths revealed a linear relationship (Fig. 4*A*; $r = -0.58$, $p = 0.01$, $n = 19$). Excluding Gly that lacks a side chain gave a slightly better fit ($r = -0.68$, $p < 0.01$, $n = 18$). The values for side chain lengths (shown in Fig. 4 legend) were estimated as the maximal lengths between the α-carbons and the most distal non-hydrogen atoms of the side chains using HyperChem 8.0 Pro (Hypercube, Inc.), which are in close agreement to the values used by Hirel *et al.* (17). For the same 18 channels (WT and mutants), I_{ss}/I_{peak} values were also found to correlate with Van der Waals' volumes (18) (Fig. 4*B*; $r = -0.54$, $p < 0.05$, $n = 18$). The correlation became insignificant when Gly was included in the analysis ($r = -0.43$, $p = 0.06$, $n = 19$). A weak correlation between I_{ss}/I_{peak} and accessible area (19) ($r = -0.49$, $p < 0.05$, $n = 18$) was also identified. No correlation between I_{ss}/I_{peak} and hydrophobicity (20) was found ($r = -0.04$, $p = 0.86$, $n = 18$). These correlation analyses suggest that the residue volume or side chain length may dictate, in part, the functionality of γMet^{438} in Na^+ self-inhibition.

Substitutions at αGly^{481} Enhance Na^+ Self-inhibition—A functional ENaC complex typically contains all three homologous subunits and, similar to cASIC1, is likely a heterotrimer (14). We examined the role of residues in α and β ECDs at the position homologous to γMet^{438} in Na^+ self-inhibition. Residue βAla^{422} was substituted with Met and Cys, whereas αGly^{481} was replaced with Met, Ala, and Cys (Fig. 5). All three α mutations (αG481A, αG481C, and αG481M) greatly enhanced Na^+ self-inhibition. The βA422C mutant showed a WT-like Na^+ self-inhibition response. Although the tau and I_{ss}/I_{peak} values for βA422M mutant were statistically greater than WT ($p < 0.05$), the changes were small compared with α and γ mutants. These results suggest that αGly^{481} plays a role in restricting Na^+ self-inhibition, and βAla^{422} is not important for this process.

Enhanced Na^+ Self-inhibition of αG481M Does Not Appear to Originate from Increased Na^+ Binding Affinity—To determine whether the altered Na^+ self-inhibition responses resulted from changed Na^+ binding affinity or allosteric steps following Na^+ binding, we examined the apparent Na^+ affinity

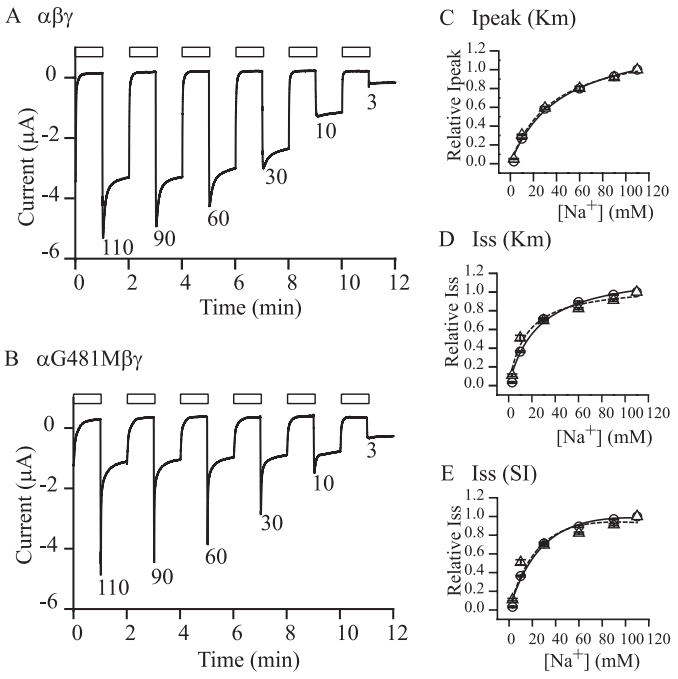

FIGURE 6. **Na^+ concentration dependence of self-inhibition.** Na^+ self-inhibition responses were examined in individual oocytes expressing WT or αG481Mβγ with extracellular Na^+ concentrations of 110, 90, 60, 30, 10, or 3 mM. *A* and *B*, representative recordings of current changes in response to the alterations of external Na^+ concentration were from five oocytes expressing αβγ and eight oocytes expressing αG481Mβγ. The *open bars* indicate the periods of time when the cell was bathed in a 1 mM NaCl solution. The *numbers* below each current decay are the Na^+ concentrations (in mM) used for inducing self-inhibition. Averaged data are shown in *C–E* with *circles* for αβγ and *triangles* for αG481M mutant. *Solid* (αβγ) and *dashed* (αG481M) *lines* were from best fitting of the relative I_{peak} (*C*) or relative I_{ss} (*D* and *E*) with equations indicated in parentheses (K_m, Michaelis equation, and SI, substrate inhibition equation, see "Experimental Procedures"). Relative I_{peak} represents the individual peak current at a specific Na^+ concentration that was normalized to the maximal I_{peak} observed in the same cell. Relative I_{ss} represents the individual steady state current normalized to maximal I_{ss} measured in the same cell.

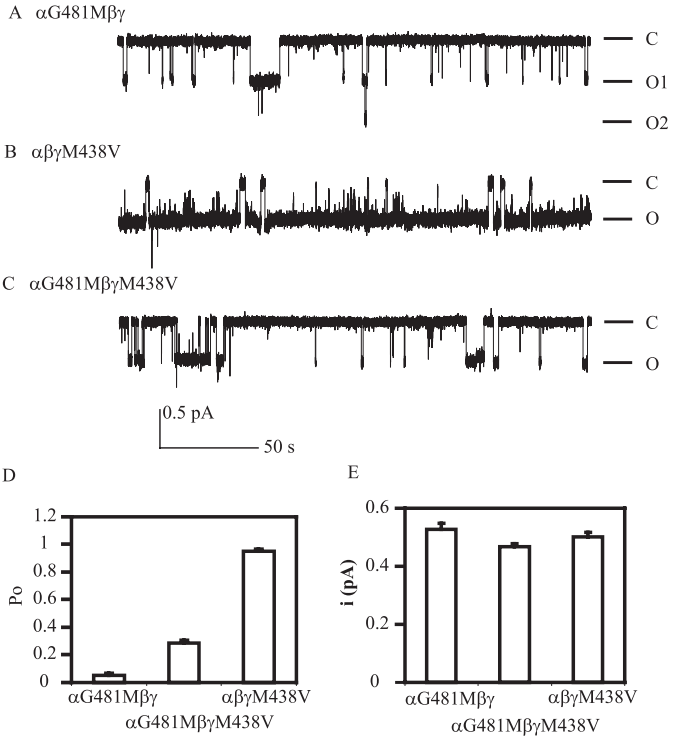

FIGURE 7. **αG418M and γM438V mutants alter P_o.** Patch clamp recordings were performed with oocytes expressing αG481Mβγ, αβγM438V and αG481M/βγM438V mENaCs. Cell-attached patches were clamped at −100 mV (membrane potential). Both bath and pipette solutions contained 110 mM Na^+. Recordings containing two or three levels of currents (one or two channels) and lasting at least 3 min were selected for analyses. Representative recordings of single channel currents are shown in *A–C*. Downward deflections indicate channel opening. The *letters C* and *O* represent closed and open states, respectively. The *scale bars* are for all three traces. The recordings were filtered at 100 Hz with low pass Gaussian algorithm by ClampFit 10 (Molecular Devices) for display. *D*, averaged P_o of the mutant channels. P_o was estimated using the single channel analysis function of ClampFit 10. The values between any two groups were significantly different ($p < 0.001$). *E*, averaged unitary currents at −100 mV. The unitary currents in each patch were obtained from the event analyses following single channel searching by ClampFit 10. The values between any two groups were not significantly different ($p > 0.05$).

for Na^+ self-inhibition. As previously described (4), we analyzed the Na^+ self-inhibition responses at 3, 10, 30, 60, 90, and 110 mM Na^+ (Fig. 6). Because Na^+ self-inhibition is a low affinity regulatory process with reported K_i over 100 mM for human and mouse ENaCs (4, 7), we chose a mutant with greatly enhanced Na^+ self-inhibition, αG481M, for this analysis. Although WT channels showed clear current decay starting from 30 mM Na^+, the αG481M displayed robust self-inhibition at Na^+ concentrations as low as 10 mM. The peak currents of both WT and mutant channels followed Michaelis-Menten enzyme kinetics very well (r^2 of 0.99; Fig. 6*C*). The estimated K_m values were slightly different (44.3 ± 0.9 mM, $n = 5$, for WT and 37.3 ± 1.9 mM, $n = 8$, for αG491M, $p < 0.05$). The steady state currents also fit well to the Michaelis equation (r^2 of 0.98 for WT and 0.97 for the mutant (Fig. 6*D*)). The estimated K_m for I_{ss} of αG481M was 15.8 ± 1.5 mM ($n = 8$), moderately lower than that of WT (25.7 ± 1.3 mM ($n = 5, p < 0.001$). We estimated the K_i of Na^+ by fitting I_{ss} against [Na^+] with the substrate inhibition equation (16) as described under "Experimental Procedures." The average K_i for αG481M mutant was 273 ± 41 mM ($n = 8$, r^2 of 0.92), not significantly different ($p > 0.05$) from that of WT (272 ± 27 mM, $n = 5$, r^2 of 0.99). Our data are consistent with the view that the enhanced Na^+ self-inhibition observed with the αG481M mutant is not due to a large change in Na^+ binding affinity but primarily reflects allosteric changes subsequent to Na^+ binding.

Mutations Affecting Na^+ Self-inhibition Alter Open Probability—Because Na^+ self-inhibition is considered an intrinsic gating event (6, 21, 22), changes in Na^+ self-inhibition observed with αGly^{481} and γMet^{438} mutant channels are expected to be associated with parallel changes in channel P_o. Unitary Na^+ currents were obtained from cell-attached patches in oocytes expressing αG481Mβγ, αβγM438V, or αG481M/βγM438V mENaCs. Both bath and pipette solutions contained 110 mM Na^+. As shown in Fig. 7, αG481Mβγ channels reside primarily in the closed state with infrequent short openings, resulting in a very low mean P_o (0.05 ± 0.01, $n = 6$). In contrast, αβγM438V channels spend most of the time in the open state with rare short closures, leading to a very high P_o (0.95 ± 0.02, $n = 6$). The double mutants behave like WT mENaC with the estimated P_o of 0.29 ± 0.02 ($n = 4$), which is close to the value we reported recently under similar conditions (0.37 ± 0.06) (11, 23). All of the mutants had unitary currents (0.53 ± 0.02 pA, $n = 6$ for αG481Mβγ; 0.50 ± 0.01 pA, $n = 6$ for

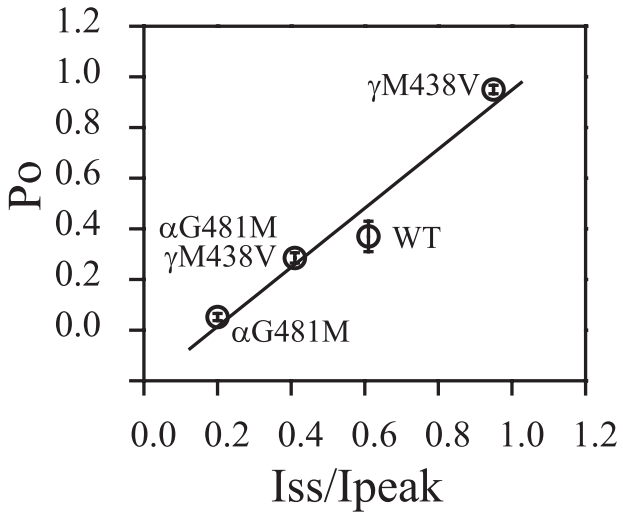

FIGURE 8. **Correlation between P_o and I_{ss}/I_{peak}.** The P_o values from Fig. 7 were plotted against the I_{ss}/I_{peak} obtained from the same mutants. The data points are labeled with mutation names. The P_o of WT was from published data (11).

$\alpha\beta\gamma$M438V and 0.47 ± 0.01 pA, $n = 4$ for αG481M/$\beta\gamma$M438V) comparable with WT (~0.5 pA) (24). A plot of P_o *versus* I_{ss}/I_{peak} values for WT (P_o for WT was obtained from Ref. 11) and the three mutants revealed a significant correlation between the two parameters ($r = 0.98$, $p < 0.05$; Fig. 8).

Both γMet^{438} and αGly^{481} Are Solvent-accessible—To further explore functional roles of αGly^{481} and γMet^{438} in the mechanism of Na^+ self-inhibition and gating of ENaC, we investigated whether they are solvent-accessible by examining the responses of the αG481C and γM438C mutants to externally applied sulfhydryl reagents. Membrane-impermeant and positively changed MTSET was chosen to avoid modifications of intracellular sulfhydryl groups (25) and because it does not significantly alter the current of WT $\alpha\beta\gamma$ mENaC (9). MTSET (1 mM) applied in the bath solution slowly inhibited currents in oocytes expressing $\alpha\beta\gamma$M438C mENaC with a maximal inhibition of 56 ± 2% ($n = 6$) within 2 min and a time constant of 40 ± 2 s ($n = 6$; Fig. 9). The inhibition persisted following washout of the reagent from the bath and was reversed by 10 mM dithiothreitol, indicating that the inhibition was due to covalent modification of the introduced Cys at γMet^{438}. The αG481C$\beta\gamma$ mutant was also inhibited by 1 mM MTSET with the maximal inhibition of 47 ± 4% ($n = 4$) within 2 min and a time constant of 3.0 ± 0.5 s ($n = 4$). MTSET caused a greater inhibition of αG481C$\beta\gamma$M438C (83 ± 1%, $n = 6$) than observed with either single mutant. The inhibition of αG481C$\beta\gamma$M438C by MTSET displayed a biphasic time course that was best described by a double exponential decay with τ_1 of 3.2 ± 0.5 s ($n = 6$) and τ_2 of 73 ± 7 s ($n = 6$). The magnitude and time course of the inhibition of αG481C$\beta\gamma$M438C by MTSET suggested that both introduced Cys residues were modified by the reagent. In contrast to αG481C and γM438C, βA422C was insensitive to external MTSET. The currents prior to MTSET, during perfusion with 1 mM MTSET, and following washout were 3.8 ± 0.2, 3.9 ± 0.2, and 3.3 ± 0.2 μA ($n = 5$), respectively ($p > 0.05$). A considerable delay following MTSET application was observed prior to current inhibition in all recordings. The estimated latencies were 3.4 ± 1.0 s ($n = 4$) for αG481C$\beta\gamma$; 7.5 ± 0.5 s ($n = 6$) for $\alpha\beta\gamma$M438C; and 3.2 ± 0.8 s ($n = 5$) for αG481C$\beta\gamma$M438C. These delays were not due to slow reagent delivery, because the oocyte perfusion rate was very high (~15 ml/min) in an oocyte chamber with unidirectional flow and small volume (~0.5 ml). In addition, the pore blocker amiloride (10 μM) had an estimated latency of 0.6 ± 0.0 s ($n = 15$, pooled from oocytes expressing all mutants).

Chemical Modification of γM438C Inhibits the Channel by "Restoring" Na^+ Self-inhibition—Current inhibition of the Cys mutants by MTSET likely reflects a decrease in channel P_o. Because P_o is correlated with the magnitude of Na^+ self-inhibition (Fig. 8), MTSET-modified $\alpha\beta\gamma$M438C should show greater Na^+ self-inhibition than unmodified $\alpha\beta\gamma$M438C. This is what we observed (Fig. 10). Following MTSET treatment, the Na^+ self-inhibition response of $\alpha\beta\gamma$M438C was greatly enhanced (I_{ss}/I_{peak} (+MTSET), 0.57 ± 0.03, $n = 5$; I_{ss}/I_{peak} (−MTSET), 0.86 ± 0.02, $n = 5$) such that the modified mutant channels behaved like WT. The modification of Cys by MTSET results in a new side chain -CH_2-S-S-$CH_2CH_2N(CH_3)_3^+$ with a length of ~9 Å (estimated using HyperChem 8.0 Pro). The linear relationship between I_{ss}/I_{peak} and side chain length (Fig. 4*A*) was preserved to a moderate degree with MTSET-modified $\alpha\beta\gamma$M438C ($r = -0.59$, $p < 0.01$, $n = 20$), supporting the notion that an increasing side chain length of residue γ438 generally favors Na^+ self-inhibition.

The introduction of a bulky side chain at the degeneration site in the ENaC pore, such as βS518K, locks the channel in an open state with a P_o close to 1 (26–31). If MTSET treatment of $\alpha\beta\gamma$M438C reduces the P_o of the channel, the channel must be able to alter transitions between open and closed states in response to MTSET. This should not occur with a mutation that locks ENaC in an open state. As shown in Fig. 11, MTSET did not alter the current in oocytes expressing $\alpha\beta$S518K/γM438C, consistent with the notion that MTSET inhibits $\alpha\beta\gamma$M438C by reducing P_o.

Mutations of Selected Aromatic Residues near αGly^{481}/γMet^{438} Alter Na^+ Self-inhibition—To examine whether residues in proximity to αGly^{481} and γMet^{438} contribute to the Na^+ self-inhibition response, we mutated four aromatic residues in the vicinity of these sites. Based on sequence alignments, these aromatic residues reside in the same helix (α5) as αGly^{481} and γMet^{438} (Fig. 1). Mutations immediately before and after αGly^{481} (αW480A and αY482A) had no significant effect on Na^+ self-inhibition (Fig. 12). However, both αY484A and αY485A greatly enhanced Na^+ self-inhibition. Substitutions immediately before and after γMet^{438} (γW437A and γY439A) significantly reduced and slowed Na^+ self-inhibition. WT-like Na^+ self-inhibition was observed in oocytes expressing the γY441A or γY442A mutant. The results suggest that αTyr^{484} and αTyr^{485} have similar functional roles as αGly^{481} in Na^+ self-inhibition. Similarly, γTrp^{437} and γTyr^{439} may have a functional role similar to γMet^{438}.

DISCUSSION

The tight correlation between ENaC P_o and the magnitude of Na^+ self-inhibition validates the concept that Na^+ self-inhibition is an intrinsic gating event that modulates channel P_o (6). The observed changes in the Na^+ self-inhibition response of

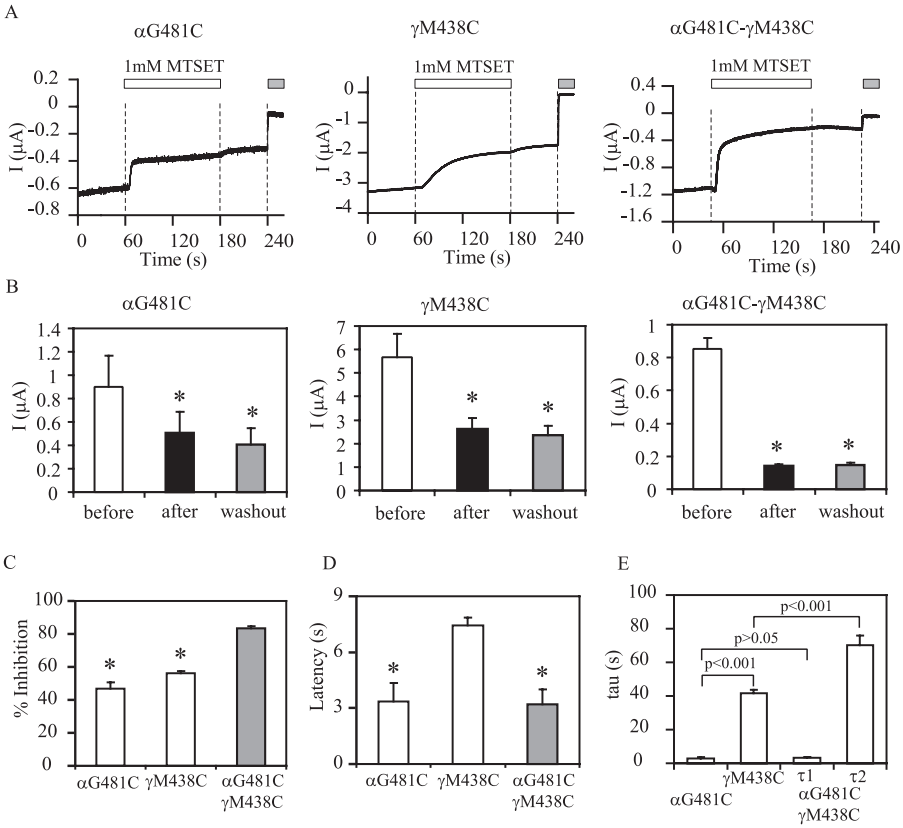

FIGURE 9. **Modification of introduced Cys at αGly^{481} and γMet^{438} by MTSET.** *A*, representative recordings showing effects of externally applied MTSET on mutant ENaCs. Whole cell currents were recorded prior to, during (*open bars*) and after bath application of 1 mM MTSET from oocytes expressing αG481Cβγ, αβγM438C, and αG481Cβγ M438C. The *gray bars* indicate the periods of time in the presence of 10 μM amiloride. The *dashed vertical lines* show the time tags generated by digital output signals that direct the perfusion valve controller to switch the bath solution. The oocytes were clamped at −60 mV for αβγM438C and −100 mV for αG481Cβγ and αG481Cβγ M438C. *B*, summary data. *White*, *black*, and *gray bars* show the averaged amiloride-sensitive currents prior to MTSET, after MTSET treatment, and following washout of MTSET, respectively. For display purposes, the inward currents (negative values) were inverted and shown as positive currents. The numbers of oocytes were 4, 7, and 6 for αG481C, αβγM438C, and αG481C-γM438C, respectively. *Asterisks* indicate that the currents were significantly different from baseline currents (prior to MTSET) ($p < 0.05$, paired *Student's t* test). *C*, percentage of MTSET-induced inhibition of the three mutants. An *asterisk* indicates that the percentage of inhibition in the single mutant was significantly lower than the double mutant ($p < 0.001$). *D*, latency. The time between the digital tag for opening the valve of the perfusion channel for MTSET and the earliest visible change in current was considered latency. An *asterisk* indicates that the value was significantly lower than that of αβγM438C ($p < 0.01$). *E*, time constants. The time constants for αG481Cβγ and αβγM438C were obtained by fitting data with a single exponential equation, whereas the τ values for αG481Cβγ M438C were from fitting with a double exponential equation.

well as to structures linking the receptors to the gate within the pore.

The changes in Na^+ self-inhibition by the homologous mutations at αGly^{481} and γMet^{438} suggest that these residues have different roles in the regulation of ENaC by external Na^+. All three αGly^{481} mutations greatly enhanced Na^+ self-inhibition, whereas most γMet^{438} mutations greatly suppressed Na^+ self-inhibition. We previously identified another pair of homologous residues, αHis^{282} and γHis^{239}, where αHis^{282} substitutions either enhanced (H282D, H282R, and H282C) or accelerated (H282W) the Na^+ self-inhibition response, whereas γHis^{239} mutations (H239D, H239R and H239C) eliminated the response (4). These observations raise the possibility that certain subdomains within the α subunit restrict Na^+ self-inhibition, whereas subdomains within the γ subunit favor Na^+ self-inhibition. Drawing parallels between the contributions of specific residues and the functional roles of different subunits should be performed with caution. For example, we recently reported that mutations at eight of sixteen extracellular Cys residues within the α subunit significantly suppressed Na^+ self-inhibition (9).

As an allosteric process, Na^+ self-inhibition likely involves three major sequential steps: Na^+ binding to its "receptor(s)," a series of local and remote conformational changes, and gate closure. αGly^{481} and γMet^{438} could contribute to one or more above steps. Because the gate of ENaC likely resides within the channel pore and the residue in cASIC1 (Lys^{342}) homologous to αGly^{481} and γMet^{438} is located at least 40 Å away from the pore domain (Fig. 1), the likelihood that either αGly^{481} or γMet^{438} is located within the gate is very low. The other two possibilities (Na^+-binding site *versus* allosteric regulatory site) are difficult to distinguish. To address this question, we estimated the apparent Na^+ affinity for Na^+ self-inhibition of WT and αG481M channels (Fig. 6). Our observations suggest that αG481M does not increase Na^+ binding affinity. Both I_{peak} and I_{ss} from WT and αG481M mutant showed similar saturation behavior that was well described by Michaelis kinetics. Because I_{peak} is observed prior to appearance of Na^+ self-inhibition, it likely represents the high P_o state of the channel, and its saturation with increasing [Na^+] largely reflects Na^+ binding affinity for the conduct-

ENaCs with mutations at γMet^{438} and/or αGly^{481} suggest that both residues have functional roles in Na^+ self-inhibition. The inhibitory effect of MTSET on channels with Cys introduced at either αGly^{481} or γMet^{438}, as well as the effects of αGly^{481} and γMet^{438} mutations on channel P_o, also supports the notion that these residues function as gating modifiers.

Our current findings provide new sites in addition to those that have previously been implicated in the allosteric regulation of ENaC by extracellular Na^+ (4, 6, 8, 9). Additional sites are expected to be identified in future studies as investigators continue to examine the mechanism of Na^+ self-inhibition, because this inhibitory response to Na^+ has a high activation energy (Q_{10} of ~8), implying that large scale conformational changes are associated with this allosteric process (7, 32). It is possible that these sites are spread out along the ECD of a subunit, contributing to one or more putative Na^+ receptors as

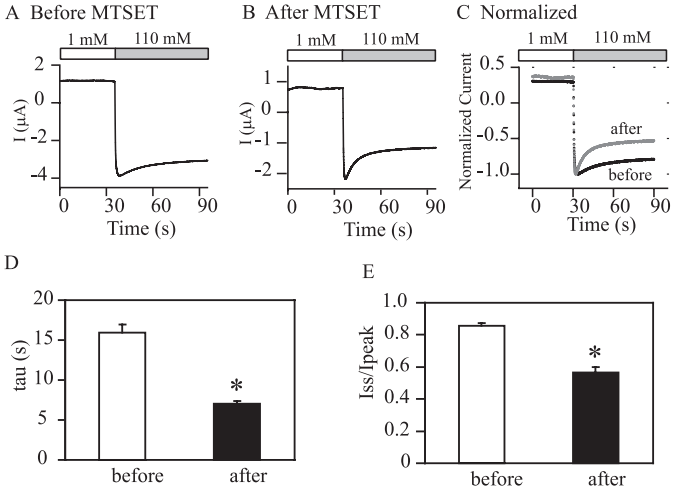

FIGURE 10. **MTSET modification of γM438C mutant enhances Na^+ self-inhibition.** Representative Na^+ self-inhibition responses in oocytes expressing αβγM438C before and after MTSET treatment are shown in *A* and *B*. Current recordings normalized to the individual peak current are shown in *C*. The *black trace* is prior to MTSET, and the *gray trace* is following MTSET. Averaged time constants and I_{ss}/I_{peak} values are shown in *D* and *E*. The values are significantly different (*asterisk*, $p < 0.01$, paired *Student's t* test, $n = 5$).

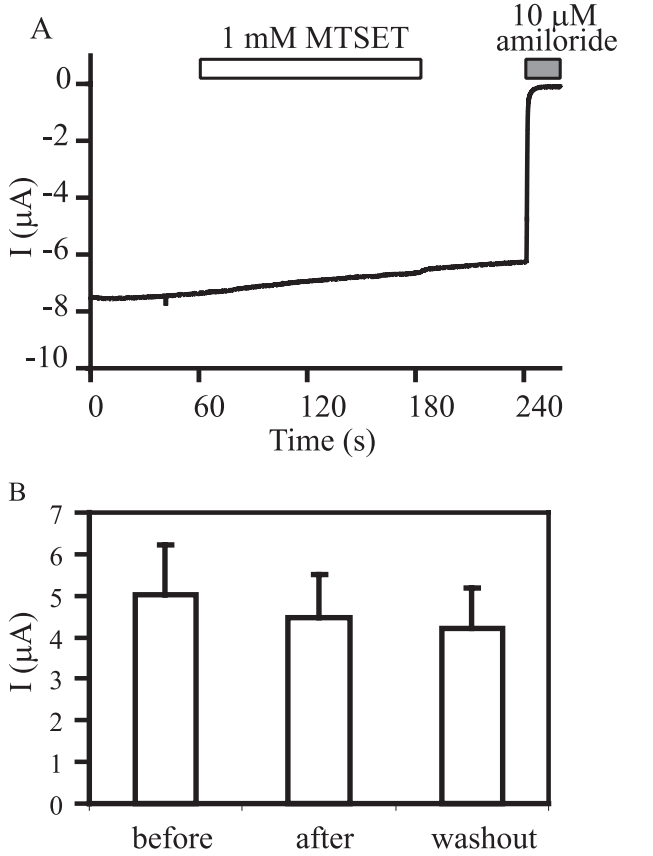

FIGURE 11. **MTSET has no effect on channels with a high intrinsic P_o.** A recording trace representing 4 independent experiments is shown in *A*. The oocyte was clamped at −60 mV 1 day after injection of cRNAs for αβS518K/γM438C mENaC. MTSET at 1 mM was applied as in Fig. 9. Amiloride-sensitive currents prior to, during (2 min) and after (1-min washout) application of MTSET are shown in *B*.

ing pore. Indeed, our estimated K_m for I_{peak} of WT mouse αβγENaC (44 mM) is very close to the K_m (48 mM) from $[Na^+]$ dependence of single channel current in rat cortical collecting

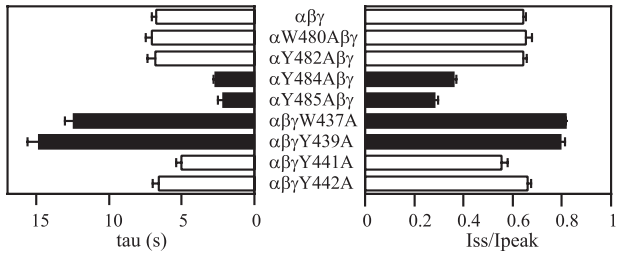

FIGURE 12. **Mutations of residues near αGly^{481}/γMet^{438} alter Na^+ self-inhibition.** The time constants and I_{ss}/I_{peak} values were obtained as described under "Experimental Procedures." The data were collected in different batches of oocytes. The WT (αβγ) values represent 27 observations from five batches of oocytes, whereas mutant data are from 7 to 12 oocytes. Student's *t* tests were performed in the same batch of oocytes to compare the Na^+ self-inhibition responses of WT and an individual mutant. The values that are significantly different from that of WT are shown as *solid bars* ($p < 0.001$).

tubule (33). On the other hand, I_{ss} saturation is influenced by Na^+ binding affinity for both the pore and the site for self-inhibition. The similar relationships of I_{peak} and I_{ss} with $[Na^+]$ suggest that the mutant and WT channels have similar Na^+ affinities for permeation and self-inhibition. If the αG481M mutant had higher Na^+ binding affinity for self-inhibition, a decline of I_{ss} at $[Na^+]$ larger than 30 mM would be expected, as we previously reported for αH282 mutants and an α furin site mutant (4, 6). Rather as seen in Fig. 6, I_{ss} for the αG481M mutant continued to increase with increasing $[Na^+]$. As a result, the $I_{ss}/[Na^+]$ data fit very well with the Michaelis equation (Fig. 6*D*). We suggest that αG481M "sensitizes" ENaC such that the conformational changes resulting from Na^+ binding are "amplified" because of a reduced energy barrier for pore closure. We did not determine the apparent Na^+ binding affinity for a γMet^{438} mutant that showed suppressed Na^+ self-inhibition, because these experiments would require a very high Na^+ concentration (≫100 mM). We speculate that γMet^{438} mutations do not alter Na^+ binding affinity based on the following observations. First, the changes in Na^+ self-inhibition with mutations of γMet^{438} are not dependent on the charge of the side chain. Second, MTSET modification of γM438C enhanced Na^+ self-inhibition. We propose that amino acid substitutions of γMet^{438} either increase or decrease the energy barrier for shutting off the channels in a residue-dependent manner. This notion is consistent with the rapid inhibition of αG481C (lowered energy barrier for closing channels) and the slow inhibition of γM438C (increased energy barrier; Fig. 9) in response to MTSET.

Our observations and insights garnered from the structure of cASIC1 allow us to address the potential functional roles of αGly^{481} and γMet^{438}. αGly^{481} appears to restrict the extent of Na^+ self-inhibition, perhaps functioning as a "brake" in the response to external Na^+. The functional role of αGly^{481} may be related to the unique properties of Gly within α-helices. Gly and Pro have the lowest helical propensity. Gly may destabilize a helical conformation by reducing the available hydrogen bonds (34, 35). In contrast, Gly residues have an important role in helix-helix packing interactions (36). For example, Gly zipper motifs (G*XX*G*XXX*G or G*XXX*G*XXX*G) are found in membrane proteins, including ion channels, and may facilitate helix packing (37). Therefore, Gly can be either a destabilizing force within a helix or serve as a stabilizing component in helical

packing. Based on the location of homologous residues Lys^{342} within cASIC1 (Fig. 1*A*), it is unlikely that αGly^{481} is involved in packing against an adjacent helix (*i.e.* $\alpha 4$ in the thumb domain or $\alpha 3$ in the finger domain). We speculate that αGly^{481} may destabilize the helical structure of $\alpha 5$ in the α subunit, reducing Na^+-induced movement of the thumb domain that leads to pore closure. Replacement of Gly by a residue that stabilizes $\alpha 5$ (Met, Cys, or Ala) would tend to enhance Na^+-induced movement of thumb domain.

The effects of substitutions of γMet^{438} on Na^+ self-inhibition correlated, in some degree, with residue volume and the length of the side chain (Fig. 4). This relationship is consistent with a "chain length effect" that has been found in the inactivation of certain enzymes and receptors (38). A long and flexible side chain (Met, Lys, or Leu) generally facilitated the functional response to external Na^+, whereas a shorter side chain (Val, Ala, Thr, Asp, Cys, or Ser) hindered the functional response. It is important to recognize that this correlation is weak, given the low correlation coefficient, and there is a clear outliner, Gly. Because Gly does not have a side chain and an introduced Gly has the possibility to alter the backbone and secondary structure, it is often difficult to predict the outcome of a Gly substitution. Clearly the side chain length (or volume) is only one of the factors that define the functional role of $\gamma 438$ in the Na^+ self-inhibition response. Side chain chemical properties such as hydrophobicity and charge do not seem to be important. For instance, substitution of γMet^{438} with negatively charged Glu or positively charged Arg suppressed Na^+ self-inhibition to a similar degree.

In contrast to the sensitivity of αGly^{481} and γMet^{438} to substitutions, the $\beta A422M$ mutant had a modestly suppressed Na^+ self-inhibition response, and $\beta A422C$ caused no change in the response. In addition, $\alpha\beta A422C\gamma$ was not sensitive to external MTSET. This is reminiscent of previous observations that mutations of β residues often resulted in little or no effect on the Na^+ self-inhibition response, whereas large changes in Na^+ self-inhibition were seen with substitutions of the corresponding residues in the α or γ subunit (4, 9). These results suggest that the β subunit has, at best, a limited role in Na^+ self-inhibition of channels composed of all three subunits. However, the β subunit clearly contributes to the gating mechanism of ENaC, because dramatic changes of P_o have been reported with mutations or modifications of an introduced Cys at the degeneration site in the β subunit (26, 28, 29, 31).

One intriguing feature of the thumb domain $\alpha 5$ is that there are four well conserved aromatic residues in the neighborhood of $\alpha Gly^{481}/\gamma Met^{438}$ and the $\alpha Cys^{483}/\gamma Cys^{440}$ (the 13^{th} Cys within the ECDs). Previous studies using crystallographic data have suggested that there exists a strong sulfur-aromatic interaction that may contribute to protein stability (39). Our mutational analyses indicate that $\alpha G481A$, $\alpha Y484A$, and $\alpha Y485A$ have a similar phenotype (*i.e.* enhancement on Na^+ self-inhibition), suggesting a shared functional role. Equivalently, $\gamma W437A$, $\gamma M438A$, and $\gamma Y439A$ may contribute to Na^+ self-inhibition in a similar manner.

In summary, we have identified two homologous residues ($\alpha Gly^{481}/\gamma Met^{438}$) in the extracellular thumb domains of α and γ ENaC subunits as novel structural determinants for Na^+ self-inhibition and gating. A long side chain (or no side chain (*i.e.* Gly)) at position $\gamma 438$ appears to preserve the functional role of Met^{438}, whereas Gly at position $\alpha 481$ restricts the degree of Na^+ self-inhibition. A strong correlation between P_o and the magnitude of Na^+ self-inhibition was observed. Experiments from sulfhydryl modifications demonstrated that both residues are accessible to extracellular solvent. Our results support the notion that the putative helices of ENaC homologous to the $\alpha 5$ of the thumb domains in the cASIC1 structure are important components of the allosteric pathway for ENaC gating and its regulation by extracellular Na^+.

Acknowledgment—We thank Dr. Ossama B. Kashlan for helpful discussion on data analysis.

REFERENCES

1. Rossier, B. C., Pradervand, S., Schild, L., and Hummler, E. (2002) *Annu. Rev. Physiol.* **64,** 877–897
2. Garty, H., and Palmer, L. G. (1997) *Physiol. Rev.* **77,** 359–396
3. Sheng, S., Johnson, J. P., and Kleyman, T. R. (2007) in *Seldin and Giebisch's The Kidney: Physiology & Pathophysiology* (Alpern, R. J., and Hebert, S. C. eds.), 4th Ed., pp. 743–768, Academic Press, New York
4. Sheng, S., Bruns, J. B., and Kleyman, T. R. (2004) *J. Biol. Chem.* **279,** 9743–9749
5. Horisberger, J. D., and Chraibi, A. (2004) *Nephron. Physiol.* **96,** p37–41
6. Sheng, S., Carattino, M. D., Bruns, J. B., Hughey, R. P., and Kleyman, T. R. (2006) *Am. J. Physiol.* **290,** F1488–F1496
7. Chraibi, A., and Horisberger, J. D. (2002) *J. Gen. Physiol.* **120,** 133–145
8. Babini, E., Geisler, H. S., Siba, M., and Grunder, S. (2003) *J. Biol. Chem.* **278,** 28418–28426
9. Sheng, S., Maarouf, A. B., Bruns, J. B., Hughey, R. P., and Kleyman, T. R. (2007) *J. Biol. Chem.* **282,** 20180–20190
10. Hughey, R. P., Bruns, J. B., Kinlough, C. L., Harkleroad, K. L., Tong, Q., Carattino, M. D., Johnson, J. P., Stockand, J. D., and Kleyman, T. R. (2004) *J. Biol. Chem.* **279,** 18111–18114
11. Bruns, J. B., Carattino, M. D., Sheng, S., Maarouf, A. B., Weisz, O. A., Pilewski, J. M., Hughey, R. P., and Kleyman, T. R. (2007) *J. Biol. Chem.* **282,** 6153–6160
12. Adebamiro, A., Cheng, Y., Rao, U. S., Danahay, H., and Bridges, R. J. (2007) *J. Gen. Physiol.* **130,** 611–629
13. Bize, V., and Horisberger, J. D. (2007) *Am. J. Physiol.* **293,** F1137–F1146
14. Jasti, J., Furukawa, H., Gonzales, E. B., and Gouaux, E. (2007) *Nature* **449,** 316–323
15. Sheng, S., Li, J., McNulty, K. A., Avery, D., and Kleyman, T. R. (2000) *J. Biol. Chem.* **275,** 8572–8581
16. Schulz, A. R. (1994) *Enzyme Kinetics: From Disease to Multi-enzyme Systems*, pp. 38–41, Cambridge University Press, Cambridge, UK
17. Hirel, P. H., Schmitter, M. J., Dessen, P., Fayat, G., and Blanquet, S. (1989) *Proc. Natl. Acad. Sci. U. S. A.* **86,** 8247–8251
18. Creighton, T. E. (1993) *Proteins: Structures and Molecular Properties*, p. 4, W. H. Freeman, New York, NY
19. Chothia, C. (1976) *J. Mol. Biol.* **105,** 1–12
20. Kyte, J., and Doolittle, R. F. (1982) *J. Mol. Biol.* **157,** 105–132
21. Van Driessche, W., and Zeiske, W. (1985) *Physiol. Rev.* **65,** 833–903
22. Garty, H., and Benos, D. J. (1988) *Physiol. Rev.* **68,** 309–373
23. Carattino, M. D., Sheng, S., and Kleyman, T. R. (2005) *J. Biol. Chem.* **280,** 4393–4401
24. Sheng, S., Perry, C. J., and Kleyman, T. R. (2002) *J. Biol. Chem.* **277,** 50098–50111
25. Kellenberger, S., Gautschi, I., Pfister, Y., and Schild, L. (2005) *J. Biol. Chem.* **280,** 7739–7747
26. Snyder, P. M., Bucher, D. B., and Olson, D. R. (2000) *J. Gen. Physiol.* **116,** 781–790
27. Sheng, S., Li, J., McNulty, K. A., Kieber-Emmons, T., and Kleyman, T. R.

(2001) *J. Biol. Chem.* **276,** 1326–1334
28. Kellenberger, S., Gautschi, I., and Schild, L. (2002) *J. Physiol.* **543,** 413–424
29. Condliffe, S. B., Zhang, H., and Frizzell, R. A. (2004) *J. Biol. Chem.* **279,** 10085–10092
30. Carattino, M. D., Edinger, R. S., Grieser, H. J., Wise, R., Neumann, D., Schlattner, U., Johnson, J. P., Kleyman, T. R., and Hallows, K. R. (2005) *J. Biol. Chem.* **280,** 17608–17616
31. Carattino, M. D., Sheng, S., Bruns, J. B., Pilewski, J. M., Hughey, R. P., and Kleyman, T. R. (2006) *J. Biol. Chem.* **281,** 18901–18907
32. Chraibi, A., and Horisberger, J. D. (2003) *Pflugers Arch. Eur. J. Physiol.* **447,** 316–320
33. Palmer, L. G., Sackin, H., and Frindt, G. (1998) *J. Physiol.* **509,** 151–162
34. Pace, C. N., and Scholtz, J. M. (1998) *Biophys. J.* **75,** 422–427
35. Senes, A., Engel, D. E., and DeGrado, W. F. (2004) *Curr. Opin. Struct. Biol.* **14,** 465–479
36. Curran, A. R., and Engelman, D. M. (2003) *Curr. Opin. Struct. Biol.* **13,** 412–417
37. Kim, S., Jeon, T. J., Oberai, A., Yang, D., Schmidt, J. J., and Bowie, J. U. (2005) *Proc. Natl. Acad. Sci. U. S. A.* **102,** 14278–14283
38. Shahrestanifar, M. S., and Howells, R. D. (1996) *Neurochem. Res.* **21,** 1295–1299
39. Zauhar, R. J., Colbert, C. L., Morgan, R. S., and Welsh, W. J. (2000) *Biopolymers* **53,** 233–248